Observation of the $h_c(1P)$ Using e^+e^- Collisions above the $D\bar{D}$ Threshold

T. K. Pedlar,[1] D. Cronin-Hennessy,[2] J. Hietala,[2] S. Dobbs,[3] Z. Metreveli,[3] K. K. Seth,[3] A. Tomaradze,[3] T. Xiao,[3] L. Martin,[4] A. Powell,[4] G. Wilkinson,[4] H. Mendez,[5] J. Y. Ge,[6] D. H. Miller,[6] I. P. J. Shipsey,[6] B. Xin,[6] G. S. Adams,[7] D. Hu,[7] B. Moziak,[7] J. Napolitano,[7] K. M. Ecklund,[8] J. Insler,[9] H. Muramatsu,[9] C. S. Park,[9] L. J. Pearson,[9] E. H. Thorndike,[9] S. Ricciardi,[10] C. Thomas,[4,10] M. Artuso,[11] S. Blusk,[11] R. Mountain,[11] T. Skwarnicki,[11] S. Stone,[11] L. M. Zhang,[11] G. Bonvicini,[12] D. Cinabro,[12] A. Lincoln,[12] M. J. Smith,[12] P. Zhou,[12] J. Zhu,[12] P. Naik,[13] J. Rademacker,[13] D. M. Asner,[14,*] K. W. Edwards,[14] K. Randrianarivony,[14] G. Tatishvili,[14,*] R. A. Briere,[15] H. Vogel,[15] P. U. E. Onyisi,[16] J. L. Rosner,[16] J. P. Alexander,[17] D. G. Cassel,[17] S. Das,[17] R. Ehrlich,[17] L. Gibbons,[17] S. W. Gray,[17] D. L. Hartill,[17] B. K. Heltsley,[17] D. L. Kreinick,[17] V. E. Kuznetsov,[17] J. R. Patterson,[17] D. Peterson,[17] D. Riley,[17] A. Ryd,[17] A. J. Sadoff,[17] X. Shi,[17] W. M. Sun,[17] J. Yelton,[18] P. Rubin,[19] N. Lowrey,[20] S. Mehrabyan,[20] M. Selen,[20] J. Wiss,[20] J. Libby,[21] M. Kornicer,[22] R. E. Mitchell,[22] M. R. Shepherd,[22] C. M. Tarbert,[22] and D. Besson[23]

(CLEO Collaboration)

[1]*Luther College, Decorah, Iowa 52101, USA*
[2]*University of Minnesota, Minneapolis, Minnesota 55455, USA*
[3]*Northwestern University, Evanston, Illinois 60208, USA*
[4]*University of Oxford, Oxford OX1 3RH, United Kingdom*
[5]*University of Puerto Rico, Mayaguez, Puerto Rico 00681*
[6]*Purdue University, West Lafayette, Indiana 47907, USA*
[7]*Rensselaer Polytechnic Institute, Troy, New York 12180, USA*
[8]*Rice University, Houston, Texas 77005, USA*
[9]*University of Rochester, Rochester, New York 14627, USA*
[10]*STFC Rutherford Appleton Laboratory, Chilton, Didcot, Oxfordshire, OX11 0QX, United Kingdom*
[11]*Syracuse University, Syracuse, New York 13244, USA*
[12]*Wayne State University, Detroit, Michigan 48202, USA*
[13]*University of Bristol, Bristol BS8 1TL, United Kingdom*
[14]*Carleton University, Ottawa, Ontario, Canada K1S 5B6*
[15]*Carnegie Mellon University, Pittsburgh, Pennsylvania 15213, USA*
[16]*University of Chicago, Chicago, Illinois 60637, USA*
[17]*Cornell University, Ithaca, New York 14853, USA*
[18]*University of Florida, Gainesville, Florida 32611, USA*
[19]*George Mason University, Fairfax, Virginia 22030, USA*
[20]*University of Illinois, Urbana-Champaign, Illinois 61801, USA*
[21]*Indian Institute of Technology Madras, Chennai, Tamil Nadu 600036, India*
[22]*Indiana University, Bloomington, Indiana 47405, USA*
[23]*University of Kansas, Lawrence, Kansas 66045, USA*

(Received 11 April 2011; published 20 July 2011)

Using 586 pb^{-1} of e^+e^- collision data at $E_{\mathrm{c.m.}} = 4170$ MeV, produced at the Cornell Electron Storage Ring collider and collected with the CLEO-c detector, we observe the process $e^+e^- \to \pi^+\pi^- h_c(1P)$. We measure its cross section to be $15.6 \pm 2.3 \pm 1.9 \pm 3.0$ pb, where the third error is due to the external uncertainty on the branching fraction of $\psi(2S) \to \pi^0 h_c(1P)$, which we use for normalization. We also find evidence for $e^+e^- \to \eta h_c(1P)$ at 4170 MeV at the 3σ level and see hints of a rise in the $e^+e^- \to \pi^+\pi^- h_c(1P)$ cross section at 4260 MeV.

DOI: 10.1103/PhysRevLett.107.041803 PACS numbers: 13.20.Gd

In a previous Letter [1], the CLEO Collaboration investigated 15 transitions to the J/ψ, $\psi(2S)$, and χ_{cJ} of charmonium states produced in e^+e^- collisions with $E_{\mathrm{c.m.}} = 3970$–4260 MeV. The data were grouped into three energy bins (3970–4060, 4120–4200, and 4260 MeV) roughly corresponding to the $\psi(4040)$, $\psi(4160)$, and $Y(4260)$ regions, respectively. Increases in the $e^+e^- \to \pi^+\pi^- J/\psi$ and $e^+e^- \to \pi^0\pi^0 J/\psi$ cross sections at $E_{\mathrm{c.m.}} = 4260$ MeV were attributed to $Y(4260)$ production [2]. In this Letter, we extend those investigations to search for $\pi^+\pi^-$, $\pi^0\pi^0$, π^0, and η transitions to the h_c [where $h_c \equiv h_c(1P)$]. We use the same 60 pb^{-1} of data with $E_{\mathrm{c.m.}} = 3970$–4260 MeV (referred to as the "scan data" [3]) and the same energy binning, but we

also now use 586 pb^{-1} of data collected at $E_{\rm c.m.} = 4170$ MeV (referred to as the "4170 data"). The 4170 data set is an order of magnitude larger than was available at that energy for the previous study. The observation of transitions to the h_c could provide insight into the perplexing nature of the charmonium states above the $D\bar{D}$ threshold [4]. It has also inspired new ways to search for and study bottomonium states, such as the h_b [5,6].

We search for the processes $e^+e^- \to Xh_c$ ($X \equiv \pi^+\pi^-, \pi^0\pi^0, \pi^0, \eta$) by reconstructing the h_c through $\gamma\eta_c$ and the η_c through $2(\pi^+\pi^-)$, $2(\pi^+\pi^-)2\pi^0$, $3(\pi^+\pi^-)$, $K^\pm K^0_S\pi^\mp$, $K^\pm K^0_S\pi^\mp\pi^+\pi^-$, $K^+K^-\pi^0$, $K^+K^-\pi^+\pi^-$, $K^+K^-\pi^+\pi^-\pi^0$, $K^+K^-2(\pi^+\pi^-)$, $2(K^+K^-)$, $\eta\pi^+\pi^-$, and $\eta 2(\pi^+\pi^-)$, the same 12 modes used in the CLEO measurement of $\mathcal{B}(J/\psi \to \gamma\eta_c)$ [7]. We also use a data sample of 24.5×10^6 $\psi(2S)$ decays to reconstruct the process $\psi(2S) \to \pi^0 h_c$ by using the same method. To eliminate dependence on the branching fractions of the η_c, we take ratios of the cross sections (σ^X_E) for $e^+e^- \to Xh_c$ at center-of-mass energy E to the branching fraction ($\mathcal{B}^{\pi^0}_\psi$) of $\psi(2S) \to \pi^0 h_c$. We use $\mathcal{B}^{\pi^0}_\psi = (8.4 \pm 1.3 \pm 1.0) \times 10^{-4}$, measured by BESIII [8], to obtain σ^X_E.

We utilize symmetric e^+e^- collisions provided by the Cornell Electron Storage Ring with center-of-mass energies at the $\psi(2S)$ mass and in the range 3970–4260 MeV. The resulting final state particles ($K^\pm$, $\pi^\pm$, and γ) are detected by the CLEO-c detector [9], which has a solid angle coverage of 93%. The momenta of charged particles are measured by concentric drift chambers [10], operating in a 1.0 T magnetic field along the beam axis, with relative momentum resolutions of $\approx 0.6\%$ at $p = 1$ GeV/c. To separate $K^\pm$ from $\pi^\pm$, two particle identification systems are used—one based on ionization energy loss (dE/dx) in the drift chamber and the other a ring-imaging Cherenkov detector [11]. Photon energies are measured with a cesium iodide calorimeter, which has relative energy resolutions of 2.2% at $E_\gamma = 1$ GeV and 5% at 100 MeV.

We use standard track quality, particle identification, and calorimetry selection requirements [7] to reconstruct the exclusive processes $e^+e^- \to Xh_c$ and $\psi(2S) \to \pi^0 h_c$ with $h_c \to \gamma\eta_c$. The η's from the η_c are reconstructed in both their $\gamma\gamma$ and $\pi^+\pi^-\pi^0$ decay modes, but the transition η from $e^+e^- \to \eta h_c$ is reconstructed only in its $\gamma\gamma$ mode (due to large combinatoric backgrounds and small efficiencies for the $\pi^+\pi^-\pi^0$ mode). For π^0 and η decays to $\gamma\gamma$, the mass of the pair of daughter photons is required to be within 3σ of the nominal mass and is subsequently constrained to that mass. To reconstruct $\eta \to \pi^+\pi^-\pi^0$, the three pions must have an invariant mass within 30 MeV/c^2 of the nominal η mass. The K^0_S candidates are selected from pairs of oppositely charged and vertex-constrained tracks (assumed to be pions) with an invariant mass within 15 MeV/c^2 of the K^0_S mass. In addition, we require that the photon from $h_c \to \gamma\eta_c$ cannot be paired with any other shower in the event to form a diphoton mass within 3σ of the π^0 mass. A four-constraint kinematic fit of all identified particles to the initial e^+e^- four-momentum is then performed, and the resulting fit quality is required to satisfy $\chi^2_{4C}/\text{d.o.f.} < 5$. This procedure sharpens the measured momenta in signal events and reduces backgrounds with missing or extra particles. For each decay mode of the η_c, the candidate with the best fit quality is accepted. The selection criteria for $\psi(2S) \to \pi^0 h_c$ are identical to that for $e^+e^- \to Xh_c$ except for an additional requirement suppressing $\psi(2S) \to \pi^+\pi^- J/\psi$ by the exclusion of any event with a $\pi^+\pi^-$ pair with a recoil mass within 15 MeV/c^2 of $M(J/\psi)$.

We select the η_c by requiring the recoil mass of the γX system to be between 2930 and 3030 MeV/c^2. We then search for the h_c in the recoil mass distribution of the X system. Figure 1 shows a histogram of the $\pi^+\pi^-$ and $\gamma\pi^+\pi^-$ recoil masses for the process $e^+e^- \to \pi^+\pi^- h_c$ at $E_{\rm c.m.} = 4170$ MeV. A clear accumulation of events can be seen near the intersection of the h_c and η_c masses, which marks the signal. Background from the initial state radiation process $e^+e^- \to \gamma\psi(2S)$; $\psi(2S) \to \pi^+\pi^- J/\psi$ appears as a vertical band at the J/ψ mass and is well-separated from the signal. Other backgrounds, studied with dedicated background Monte Carlo simulations, are smooth and are due to the light-quark continuum ($e^+e^- \to q\bar{q}$) or $D\bar{D}$ production, simulated with previously measured cross sections [3].

The yield of $e^+e^- \to \pi^+\pi^- h_c$ events at $E_{\rm c.m.} = 4170$ MeV is determined by fitting the $\pi^+\pi^-$ recoil mass distribution, after selecting the η_c, with two

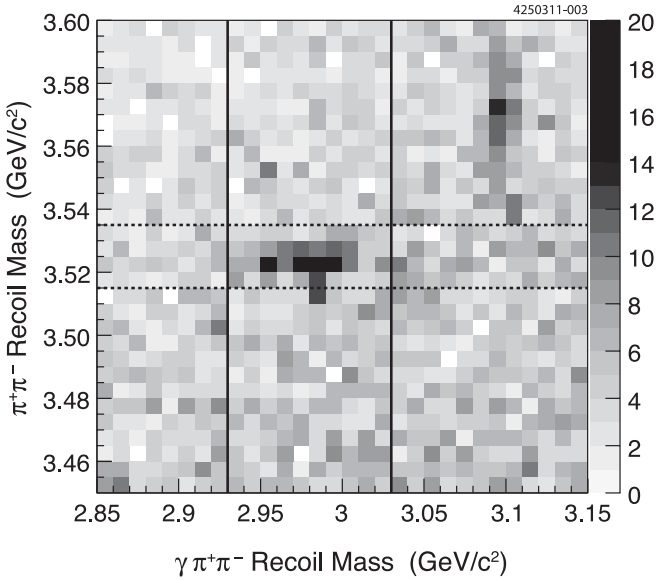

FIG. 1. The recoil mass of the $\pi^+\pi^-$ system versus the recoil mass of the $\gamma\pi^+\pi^-$ system for candidate $e^+e^- \to \pi^+\pi^- h_c$; $h_c \to \gamma\eta_c$ events at $E_{\rm c.m.} = 4170$ MeV. The signal appears at the intersection of the h_c and η_c masses. The vertical lines indicate the region used to select the η_c. The horizontal lines mark ± 10 MeV/c^2 around the h_c mass.

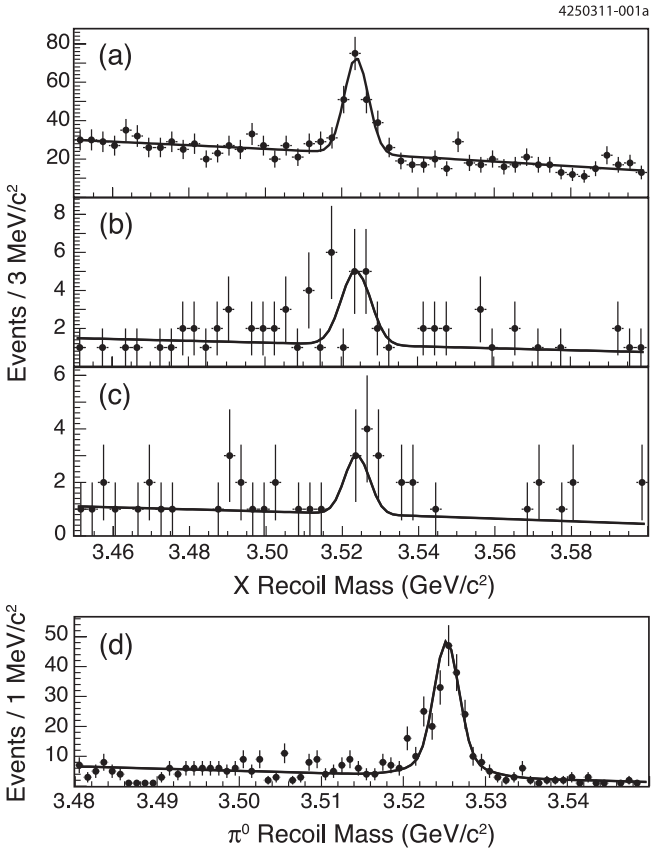

FIG. 2. Fits to determine the yields of h_c events from (a) $e^+e^- \to \pi^+\pi^- h_c$ at $E_{\rm c.m.} = 4170$ MeV; (b) $e^+e^- \to \eta h_c$ at $E_{\rm c.m.} = 4170$ MeV; (c) $e^+e^- \to \pi^+\pi^- h_c$ at $E_{\rm c.m.} = 4260$ MeV; and (d) the normalizing mode $\psi(2S) \to \pi^0 h_c$.

components. The signal shape is described by a double Gaussian with floating mass and normalization but with widths fixed by signal Monte Carlo simulations. The background shape is a freely floating first-order polynomial. The resulting fit is shown in Fig. 2(a). We find 131 ± 15 signal events with a significance of more than 10σ. The significance, here and in subsequent fits, is calculated from log-likelihood differences between fits with and without a signal component. The resulting mass from the fit is 3523.86 ± 0.48 MeV/c^2 (statistical errors only), which is 1.5 MeV/c^2 lower than the Particle Data Group 2010 value of 3525.42 ± 0.29 MeV/c^2 [12]. This discrepancy, however, is less than the uncertainty of the initial e^+e^- energy (≈ 2 MeV) used in the kinematic fit, which directly affects the measured dipion recoil mass.

Fits to $e^+e^- \to (\pi^0\pi^0/\pi^0/\eta)h_c$ at $E_{\rm c.m.} = 4170$ MeV and fits to $e^+e^- \to \pi^+\pi^- h_c$ with $E_{\rm c.m.} = 3970$–4260 MeV follow the same procedure except that, due to lower statistics, the mass is fixed to the value obtained previously: 3523.86 MeV/c^2. The resulting yields and significances are listed in Table I. We find $>3\sigma$ evidence for $e^+e^- \to \eta h_c$ at 4170 MeV [Fig. 2(b)] and hints of a signal (2.6σ) for $e^+e^- \to \pi^+\pi^- h_c$ at 4260 MeV [Fig. 2(c)].

The normalizing mode $\psi(2S) \to \pi^0 h_c$ is also fit by using the same method and with a floating mass [Fig. 2(d)]. The yield is measured to be 202 ± 16 events. The resulting mass is 3525.27 ± 0.17 MeV/c^2 (statistical errors only), consistent with, and highly correlated to, a previous measurement by CLEO using a similar method [13].

We calculate the ratios of the cross sections of $e^+e^- \to Xh_c$ at energy E (σ_E^X) to the branching fraction of $\psi(2S) \to \pi^0 h_c$ ($\mathcal{B}_\psi^{\pi^0}$) by using

$$\frac{\sigma_E^X}{\mathcal{B}_\psi^{\pi^0}} = \frac{N_\psi}{\mathcal{L}_E} \frac{N_E^X}{N_\psi^{\pi^0} R_\epsilon}, \tag{1}$$

where N_ψ is the number of $\psi(2S)$ decays, $\mathcal{L}_E$ is the luminosity at energy E, N_E^X and $N_\psi^{\pi^0}$ are measured yields, and R_ϵ is a ratio of selection efficiencies: that of $e^+e^- \to Xh_c$ to that of $\psi(2S) \to \pi^0 h_c$. Since the ratio of efficiencies for each η_c decay mode is not perfectly constant (with 10%–20% variations), we weight the individual efficiency ratios by the number of $\psi(2S) \to \pi^0 h_c$ events we observe in each η_c decay mode, which we obtain through the fitting procedure described above. The errors on the efficiency ratios include errors due to Monte Carlo statistics and errors on these individual yields.

TABLE I. Yields (N_E^X), significances, relative fitting and shape systematic errors, efficiency ratios (R_ϵ), normalized cross sections ($\sigma_E^X/\mathcal{B}_\psi^{\pi^0}$), and cross sections ($\sigma_E^X$) for each reaction $e^+e^- \to Xh_c$. The third error on σ_E^X is from $\mathcal{B}_\psi^{\pi^0}$ [8].

X	$E_{\rm c.m.}$ (MeV)	N_E^X (Events)	Sig. (σ)	Fitting Syst. (%)	Shape Syst. (%)	R_ϵ	$\sigma_E^X/\mathcal{B}_\psi^{\pi^0}$ (nb)	σ_E^X (pb)
π^0	3686 [$\psi(2S)$]	202 ± 16	>10	4.8	3.9	...	...	...
$\pi^+\pi^-$	4170	131 ± 15	>10	1.7	7.1	1.46 ± 0.04	$18.5 \pm 2.7 \pm 2.2$	$15.6 \pm 2.3 \pm 1.9 \pm 3.0$
$\pi^0\pi^0$	4170	7.4 ± 8.0	1.0	23	27	0.43 ± 0.02	$3.6 \pm 3.9 \pm 1.4$	$3.0 \pm 3.3 \pm 1.1 \pm 0.6$
π^0	4170	-5 ± 11	...	47	77	1.12 ± 0.03	$-0.9 \pm 2.1 \pm 0.8$	$-0.7 \pm 1.8 \pm 0.7 \pm 0.1$
η	4170	12.6 ± 4.5	3.8	13	11	0.47 ± 0.01	$5.6 \pm 2.1 \pm 1.1$	$4.7 \pm 1.7 \pm 1.0 \pm 0.9$
$\pi^+\pi^-$	3970–4060	0.3 ± 2.1	0.1	400	360	1.30 ± 0.04	$1.2 \pm 9.5 \pm 6.4$	$1.0 \pm 8.0 \pm 5.4 \pm 0.2$
$\pi^+\pi^-$	4120–4200	4.4 ± 3.1	1.7	52	27	1.46 ± 0.04	$13.9 \pm 9.9 \pm 8.2$	$11.7 \pm 8.3 \pm 6.9 \pm 2.3$
$\pi^+\pi^-$	4260	6.0 ± 3.1	2.6	4.9	17	1.49 ± 0.04	$38 \pm 20 \pm 8$	$32 \pm 17 \pm 6 \pm 6$

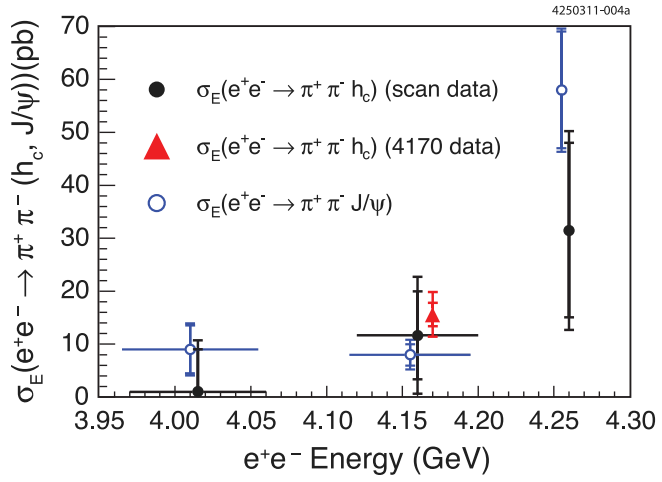

FIG. 3 (color online). Cross sections as a function of center-of-mass energy. The triangle shows the cross section for $e^+e^- \to \pi^+\pi^- h_c$ at $E_{\text{c.m.}} = 4170$ MeV; the closed circles are for the same process at other center-of-mass energies. For reference, the $e^+e^- \to \pi^+\pi^- J/\psi$ cross section [1] is indicated by open circles. The inner error bars are the statistical errors; the outer error bars are the quadratic sum of the statistical and systematic errors.

Previously determined systematic errors are used for N_ψ (2%) [14] and $\mathcal{L}_E$ (1%) [15]. Most systematic errors on individual track and photon reconstruction efficiencies cancel in the ratio of efficiencies, R_ϵ. However, for the transition particles, the X in the numerator, and the π^0 in the denominator, a 1% relative error is assigned for each track and a 2% error for each photon. A conservative 5% systematic error is included for our determination of R_ϵ, which relies upon signal Monte Carlo simulations distributed according to phase space. This systematic error is estimated by using extreme variations of the η_c substructure—for example, by replacing $2(K^+K^-)$ by $\phi(1020)\phi(1020)$.

Systematic errors in N_E^X and $N_\psi^{\pi^0}$ due to the fitting procedure are evaluated by varying the order of the background polynomials, varying the fit ranges, and varying the bin sizes. Based on Monte Carlo studies, we also use background shapes determined by χ^2_{4C}/d.o.f. sidebands ($10 < \chi^2_{4C}/\text{d.o.f.} < 35$). For $N_\psi^{\pi^0}$, we alternatively use an ARGUS distribution [16] for the background.

Systematic errors due to signal shapes are evaluated by varying the signal mass and width. The largest deviations occur when the signal widths are allowed to float. This variation determines the shape systematic error on $N_\psi^{\pi^0}$ and $N_{4170}^{\pi^+\pi^-}$. For other N_E^X, where the statistics are lower, the width variation is performed by scaling the width by the deviation observed between data and signal Monte Carlo simulations in the fit for $N_{4170}^{\pi^+\pi^-}$, which is $\approx 20\%$. Variations of the signal mass produce smaller deviations.

The final numbers are listed in Table I. The $\pi^+\pi^- h_c$ cross sections as a function of center-of-mass energy are summarized in Fig. 3. Notice that the $\pi^+\pi^- h_c$ cross sections are of a comparable size to those of $\pi^+\pi^- J/\psi$. There is also a suggestive rise in the cross section at 4260 MeV, which could be an indication of $Y(4260)$ production but will require further data to be definitive.

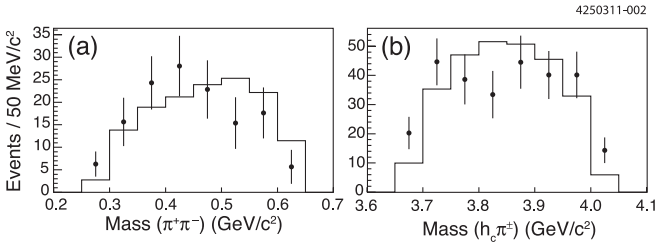

FIG. 4. The (a) $\pi^+\pi^-$ and (b) $h_c\pi^\pm$ mass distributions from $e^+e^- \to \pi^+\pi^- h_c$ at $E_{\text{c.m.}} = 4170$ MeV. The points are obtained by fitting for the h_c yields in bins of $\pi^+\pi^-$ or $\pi^\pm h_c$ mass. The histograms are from Monte Carlo simulations, generated according to phase space and scaled by the total h_c yield.

Projections of the $\pi^+\pi^- h_c$ Dalitz plot at $E_{\text{c.m.}} = 4170$ MeV are shown in Fig. 4 and are compared to phase space Monte Carlo simulations. To separate the signal from background, the number of signal $\pi^+\pi^- h_c$ events in each bin is determined by the fitting procedure described above. The efficiency is relatively uniform across the Dalitz plot. More data would be required to investigate any possible discrepancies of the data with phase space.

Assuming the $E_{\text{c.m.}} = 3970$–4060 MeV and $E_{\text{c.m.}} = 4170$ MeV data correspond to $\psi(4040)$ and $\psi(4160)$ production, respectively, we convert cross sections to upper limits on branching fractions by using the same conversion factors listed in a previous CLEO analysis of this region [1]. The results are listed in Table II. Assuming the 4260 MeV point is purely due to $Y(4260)$ production, we set a limit on its branching fraction to $\pi^+\pi^- h_c$ relative to $\pi^+\pi^- J/\psi$ of <1.0 at 90% confidence level.

In summary, we observe the process $e^+e^- \to \pi^+\pi^- h_c$ at $E_{\text{c.m.}} = 4170$ MeV and find its cross section to be comparable to the corresponding cross section for J/ψ production. This has already resulted in new methods to search for and study the h_b by using e^+e^- collisions above the $B\bar{B}$ threshold [6]. We also see hints of a rise in the $\pi^+\pi^- h_c$ cross section at $E_{\text{c.m.}} = 4260$ MeV. Further data will be required, however, to determine if this rise can be attributed to the $Y(4260)$.

TABLE II. Upper limits (at 90% confidence level) on branching fractions for the $\psi(4040)$ and $\psi(4160)$ to Xh_c.

X	$\mathcal{B}(\psi(4040) \to Xh_c)$ ($\times 10^{-3}$)	$\mathcal{B}(\psi(4160) \to Xh_c)$ ($\times 10^{-3}$)
$\pi^+\pi^-$	<3	<5
$\pi^0\pi^0$	...	<2
π^0	...	<0.4
η	...	<2

We gratefully acknowledge the effort of the Cornell Electron Storage Ring staff in providing us with excellent luminosity and running conditions. This work was supported by the A. P. Sloan Foundation, the National Science Foundation, the U.S. Department of Energy, the Natural Sciences and Engineering Research Council of Canada, and the United Kingdom Science and Technology Facilities Council.

*Present address: Pacific Northwest National Laboratory, Richland, WA 99352, USA.

[1] T. E. Coan *et al.* (CLEO Collaboration), Phys. Rev. Lett. **96**, 162003 (2006).
[2] B. Aubert *et al.* (BABAR Collaboration), Phys. Rev. Lett. **95**, 142001 (2005).
[3] D. Cronin-Hennessy *et al.* (CLEO Collaboration), Phys. Rev. D **80**, 072001 (2009).
[4] N. Brambilla *et al.*, Eur. Phys. J. C **71**, 1 (2011).
[5] J. P. Lees *et al.* (BABAR Collaboration), arXiv:1102.4565.
[6] I. Adachi *et al.* (Belle Collaboration), arXiv:1103.3419.
[7] R. E. Mitchell *et al.* (CLEO Collaboration), Phys. Rev. Lett. **102**, 011801 (2009).
[8] M. Ablikim *et al.* (BESIII Collaboration), Phys. Rev. Lett. **104**, 132002 (2010).
[9] Y. Kubota *et al.* (CLEO Collaboration), Nucl. Instrum. Methods Phys. Res., Sect. A **320**, 66 (1992).
[10] D. Peterson *et al.*, Nucl. Instrum. Methods Phys. Res., Sect. A **478**, 142 (2002).
[11] M. Artuso *et al.*, Nucl. Instrum. Methods Phys. Res., Sect. A **502**, 91 (2003).
[12] K. Nakamura *et al.* (Particle Data Group), J. Phys. G **37**, 075021 (2010).
[13] S. Dobbs *et al.* (CLEO Collaboration), Phys. Rev. Lett. **101**, 182003 (2008).
[14] H. Mendez *et al.* (CLEO Collaboration), Phys. Rev. D **78**, 011102 (2008).
[15] S. Dobbs *et al.* (CLEO Collaboration), Phys. Rev. D **76**, 112001 (2007).
[16] H. Albrecht *et al.* (ARGUS Collaboration), Phys. Lett. B **340**, 217 (1994).